ter using a Fabry–Perot interferometer," *Rev. Sci. Instr.*, vol. 34, p. 843, Aug. 1963.
[7] P. D. Potter, "A new horn antenna with suppressed sidelobes and equal beamwidths," *Microwave J.*, vol. 6, p. 71, June 1963.
[8] H. Kogelnik and T. Li, "Laser beams and resonators," *Proc. IEEE*, vol. 54, p. 172, Oct. 1966.
[9] T. Li, "Diffraction loss and selection of modes in maser resonators with circular mirrors," *Bell Syst. Tech. J.*, vol. 44, p. 917, May–June 1965.

Green's Functions for Triangular Segments in Planar Microwave Circuits

RAKESH CHADHA, STUDENT MEMBER, IEEE, AND
K. C. GUPTA, SENIOR MEMBER, IEEE

***Abstract*—Green's functions are developed for the analysis of triangular segments in microwave planar circuits. Three types of triangles (30°–60° right-angled, equilateral, and isosceles right-angled) are treated by placing additional image sources outside the triangular region.**

I. Introduction

Two-dimensional microwave planar components have been proposed for use in microwave-integrated circuits [1]–[3]. One of the methods for analyzing these components is by use of Green's functions relating voltage at any point to a line current excitation [1]. The Green's functions for rectangular and circular geometries are available [1]. Recently triangular elements have also been proposed for realizing resonators and prototype elements for bandpass and bandstop filters [4], [5]. The triangular resonators have been used in the design of 3-port circulators [5], and gap-coupled triangular segments have been proposed for use in filter circuits [4]. Also, characterization of triangular segments is necessary when an accurate analysis of a three-microstrip junction (such as encountered in power dividers), shown in Fig. 1, is needed. However, Green's functions for triangular geometries have not been reported so far. This paper describes the development of Green's functions for three kinds of triangular geometries useful in planar circuits. These are 1) a 30°–60° right-angled triangle, 2) an equilateral triangle, and 3) an isosceles right-angled triangle.

The basic integral equation involved in the analysis of planar circuits [1] is

$$V(x,y)=\int\int_D G(x,y|x_0,y_0)i(x_0,y_0)\,dx_0\,dy_0 \qquad (1)$$

where G is the Green's function of the second kind having dimension of impedance and $i(x_0,y_0)$ denotes a fictitious source current density injected normally. $V(x,y)$ denotes voltage at any point on the segment with respect to the ground plane. Equation (1) is satisfied inside the contour C (Fig. 2), and the open boundary condition on C may be written as

$$\frac{\partial V}{\partial n}=0. \qquad (2)$$

Manuscript received March 19, 1980; revised June 12, 1980. This work was supported by the Department of Electronics, Government of India, under a research grant.

The authors are with the Department of Electrical Engineering, Indian Institute of Technology, Kanpur 208016, India.

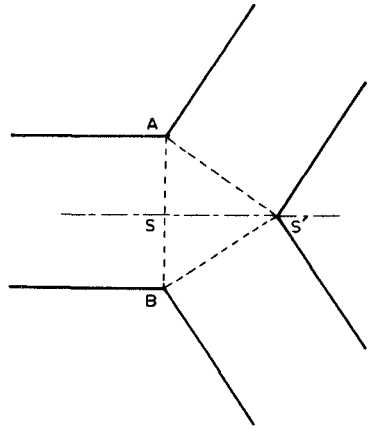

Fig. 1. Triangular segment in a typical Y junction.

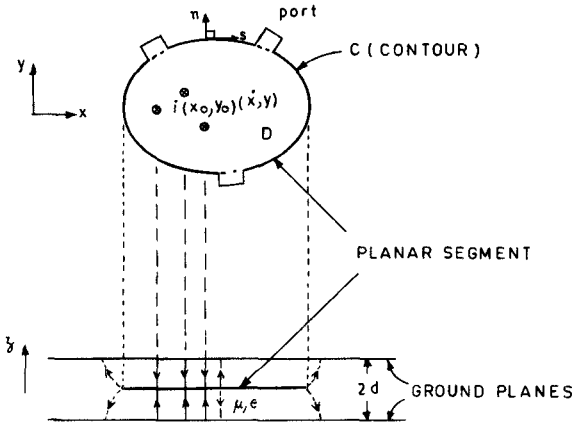

Fig. 2. Configuration for a typical segment in planar microwave circuits.

In planar circuits the dimension d is much smaller than the wavelength and the Green's function G is given by the solution of

$$(\nabla_T^2+k^2)G=-j\omega\mu d\delta(x-x_0)\delta(y-y_0) \qquad (3)$$

with

$$\partial G/\partial n=0. \qquad (4)$$

In the above, k denotes propagation constant ($\omega\sqrt{\mu\epsilon}$) in the dielectric medium. Product of delta functions $\delta(x-x_0)\delta(y-y_0)$ represents a line current flowing along z-direction and located at (x_0,y_0). Such sources have been called line sources in the text later.

In circuits, which are symmetrical about an axis, even- and odd-symmetry can be used for complete analysis of the circuit. For example, in the circuit of Fig. 1, even- and odd-mode circuits may be analyzed separately. For the odd-mode circuits, the plane of symmetry (SS' in Fig. 1) is replaced by an electric wall at which the boundary condition

$$G=0 \qquad (5)$$

must be satisfied. Thus, there is a need to obtain odd-mode Green's functions, which satisfy (5) on one side of triangle (SS') and (4) on the remaining sides (AS and AS') of the planar segment. The function G is evaluated for different triangular geometries in the following sections.

0018-9480/80/1000-1139$00.75 ©1980 IEEE

II. Green's Function for 30°–60° Right-Angle Triangle

For the triangular geometry shown in Fig. 3(a), the Green's function can be obtained by solving (3) with the boundary conditions given by (4). To obtain an analytical solution for G, the right-hand side of (3) is made periodic by placing additional line sources outside the triangle. The additional line sources can be thought of as obtained by taking multiple images [6] of the line source at (x_0, y_0) with respect to the three sides of the triangle which are magnetic walls as assumed earlier in (2). The locations of these multiple images are shown in Fig. 3(b).

It can be seen that the periodicity of the pattern is $3a$ along the y-axis and $\sqrt{3}\,a$ along the x-axis. Hence $ABCDEF$ is chosen as a basic cell which contains 24 line sources in 24 triangular regions as shown in Fig. 3(b). It may be noted that a solution for G with this set of multiple sources, will satisfy (3) in the original region of interest, since (4) is satisfied at all the boundaries of all triangular regions.

The Fourier series expressions for each of the 24-line sources, which repeat periodically in two-dimensional space, are obtained. The corresponding terms of these 24 expressions are added together and the resulting expression identical to the right-hand side of (3) in the original triangular region, can be expressed as

$$-\frac{8j\omega\mu d}{3\sqrt{3}\,a^2}\sum_{m=-\infty}^{\infty}\sum_{n=-\infty}^{\infty}\cos\left(\frac{2\pi mx}{\sqrt{3}\,a}\right)\cos\left[\frac{2\pi(m+2n)y}{3a}\right]\cdot\left\{(-1)^n\cos\left[\frac{2\pi(m+n)x_0}{\sqrt{3}\,a}\right]\cos\left[\frac{2\pi(m-n)y_0}{3a}\right]+\cos\left(\frac{2\pi mx_0}{\sqrt{3}\,a}\right)\cdot\cos\left[\frac{2\pi(m+2n)y_0}{3a}\right]+(-1)^{m+n}\cos\left(\frac{2\pi nx_0}{\sqrt{3}\,a}\right)\cdot\cos\left[\frac{2\pi(2m+n)y_0}{3a}\right]\right\}. \tag{6}$$

Now substituting $l=-(m+n)$, this reduces to

$$-\frac{8j\omega\mu d}{3\sqrt{3}\,a^2}\sum\sum(-1)^m\cos\left(\frac{2\pi mx}{\sqrt{3}\,a}\right)\cos\left[\frac{2\pi(n-l)y}{3a}\right]T_1(x_0,y_0) \tag{7}$$

where $T_1(x,y)$ is defined as

$$T_1(x,y)=(-1)^l\cos\left(\frac{2\pi lx}{\sqrt{3}\,a}\right)\cos\left[\frac{2\pi(m-n)y}{3a}\right]+(-1)^m\cos\left(\frac{2\pi mx}{\sqrt{3}\,a}\right)\cdot\cos\left[\frac{2\pi(n-l)y}{3a}\right]+(-1)^n\cos\left(\frac{2\pi nx}{\sqrt{3}\,a}\right)\cos\left[\frac{2\pi(l-m)y}{3a}\right] \tag{8}$$

with the condition that the integers l, m, and n satisfy

$$l+m+n=0. \tag{9}$$

It can be seen that

$$\sum\sum(-1)^l\cos\left(\frac{2\pi lx}{\sqrt{3}\,a}\right)\cos\left[\frac{2\pi(m-n)y}{3a}\right]T_1(x_0,y_0)=\sum\sum(-1)^m\cos\left(\frac{2\pi mx}{\sqrt{3}\,a}\right)\cos\left[\frac{2\pi(n-l)y}{3a}\right]T_1(x_0,y_0)=\sum\sum(-1)^n\cos\left(\frac{2\pi nx}{\sqrt{3}\,a}\right)\cos\left[\frac{2\pi(l-m)y}{3a}\right]T_1(x_0,y_0). \tag{10}$$

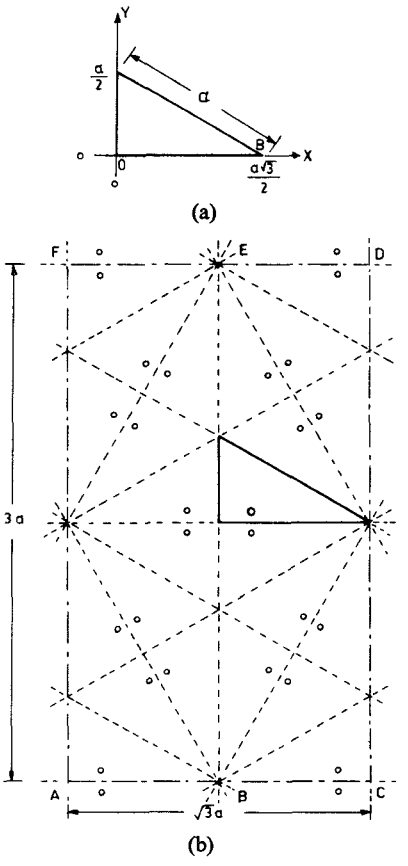

Fig. 3. (a) A 30°–60° right-angled triangular segment. (b) Location of image sources for a 30°–60° right-angled triangle.

Using (10), expression (7) can be rewritten as

$$-\frac{8j\omega\mu d}{9\sqrt{3}\,a^2}\sum\sum T_1(x_0,y_0)T_1(x,y). \tag{11}$$

It can be verified that the function $T_1(x,y)$ satisfies the boundary conditions, given by (4), for the triangle shown in Fig. 3(a). Also, it agrees with the potential function for an equilateral triangle given by Schelkunoff [7]. The Green's function G can now be written in terms of these potential functions $T_1(x,y)$ as

$$G=\sum_{m=-\infty}^{\infty}\sum_{n=-\infty}^{\infty}A_{mn}T_1(x,y). \tag{12}$$

Substituting (12) in the left-hand side of (3), we get

$$(\nabla_T^2+k^2)G=\sum_{-\infty}^{\infty}\sum_{-\infty}^{\infty}\left[k^2-\frac{16\pi^2}{9a^2}(m^2+mn+n^2)\right]A_{mn}T_1(x,y). \tag{13}$$

Since (13) and (11) are equal for all values of x and y, we have by comparison

$$A_{mn}=\frac{8j\omega\mu dT_1(x_0,y_0)}{16\sqrt{3}\,\pi^2(m^2+mn+n^2)-9\sqrt{3}\,a^2k^2}. \tag{14}$$

Substituting (14) in (12) we have

$$G(x,y|x_0,y_0)=8j\omega\mu d\cdot\sum_{-\infty}^{\infty}\sum_{-\infty}^{\infty}\frac{T_1(x_0,y_0)T_1(x,y)}{16\sqrt{3}\,\pi^2(m^2+mn+n^2)-9\sqrt{3}\,a^2k^2} \tag{15}$$

which is the required Green's function for (3), for the 30°–60° right-angle triangle shown in Fig. 3(a).

III. Green's Function for an Equilateral Triangle

As in Section II, the right-hand side of (3) can be made periodic by placing additional line sources outside the equilateral triangle shown in Fig. 4(a). The positions of additional line sources are obtained by taking multiple images of the original line source at (x_0, y_0) with respect to magnetic walls at the three sides of the triangle. In this case the basic cell which repeats itself is *ABCDEF* which contains 12-line sources in 12 triangular regions as shown in Fig. 4(b). Adding the corresponding terms in Fourier series expressions for each of the line sources in basic cell, the resulting expression equivalent to the right-hand side of (3) can be expressed as

$$
\begin{aligned}
&-\frac{4j\omega\mu d}{3\sqrt{3}\,a^2}\sum\sum\left[\cos\left(\frac{2\pi mx}{\sqrt{3}\,a}\right)\cos\left[\frac{2\pi(m+2n)y}{3a}\right]\right.\\
&\cdot\left\{(-1)^n\cos\left[\frac{2\pi(m+n)x_0}{\sqrt{3}\,a}\right]\cos\left[\frac{2\pi(m-n)y_0}{3a}\right]\right.\\
&+\cos\left(\frac{2\pi mx_0}{\sqrt{3}\,a}\right)\cos\left[\frac{2\pi(m+2n)y_0}{3a}\right]+(-1)^{m+n}\cos\left(\frac{2\pi nx_0}{\sqrt{3}\,a}\right)\\
&\cdot\cos\left[\frac{2\pi(2m+n)y_0}{3a}\right]\Bigg\}+\cos\left(\frac{2\pi mx}{\sqrt{3}\,a}\right)\sin\left[\frac{2\pi(m+2n)y}{3a}\right]\\
&\cdot\left\{\cos\left(\frac{2\pi mx_0}{\sqrt{3}\,a}\right)\sin\left[\frac{2\pi(m+2n)y_0}{3a}\right]\right.\\
&-(-1)^{m+n}\cos\left(\frac{2\pi nx_0}{\sqrt{3}\,a}\right)\sin\left[\frac{2\pi(2m+n)y_0}{3a}\right]\\
&\left.\left.+(-1)^n\cos\left[\frac{2\pi(m+n)x_0}{\sqrt{3}\,a}\right]\sin\left[\frac{2\pi(m-n)y_0}{3a}\right]\right\}\right].
\end{aligned}
\tag{16}
$$

Now substituting, $l=-(m+n)$ and simplifying as in Section II, expression (16) can be expressed as

$$
-\frac{4j\omega\mu d}{9\sqrt{3}\,a^2}\sum\sum[T_1(x_0,y_0)T_1(x,y)+T_2(x_0,y_0)T_2(x,y)] \tag{17}
$$

where $T_2(x,y)$ is defined as

$$
\begin{aligned}
T_2(x,y)=&(-1)^l\cos\left(\frac{2\pi lx}{\sqrt{3}\,a}\right)\sin\left[\frac{2\pi(m-n)y}{3a}\right]+(-1)^m\\
&\cdot\cos\left(\frac{2\pi mx}{\sqrt{3}\,a}\right)\sin\left[\frac{2\pi(n-l)y}{3a}\right]\\
&+(-1)^n\cos\left(\frac{2\pi nx}{\sqrt{3}\,a}\right)\sin\left[\frac{2\pi(l-m)y}{3a}\right].
\end{aligned}
\tag{18}
$$

The integers l, m, and n in (18) may be chosen, as in the case of $T_1(x,y)$, to satisfy (9). It can be verified that the function $T_1(x,y)$ and $T_2(x,y)$ both satisfy the boundary conditions (4) for the equilateral triangle geometry shown in Fig. 4(a). It is seen that $T_1(x,y)$ has even symmetry about the x-axis and $T_2(x,y)$ has odd symmetry about the x-axis. Since the line current excitation in the right-hand side of (3) is asymmetric, the function G should contain terms of both $T_1(x,y)$ and $T_2(x,y)$. Let

$$
G=\sum\sum[A_{mn}T_1(x,y)+B_{mn}T_2(x,y)]. \tag{19}
$$

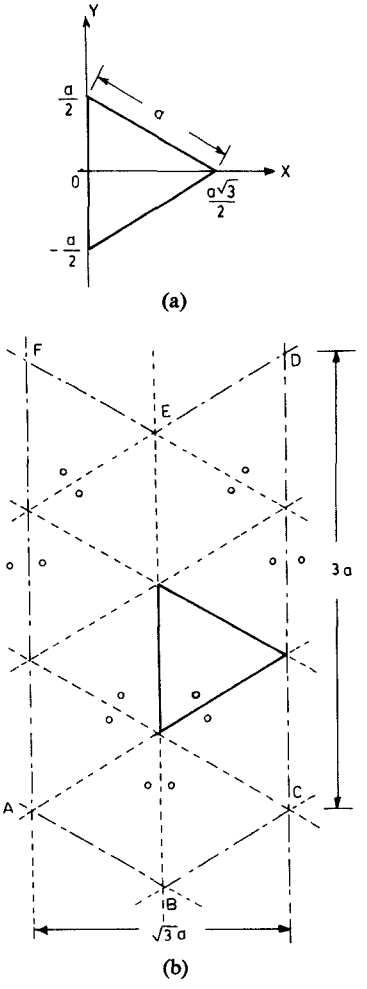

Fig. 4. (a) An equilateral triangular segment. (b) Location of image sources for an equilateral triangle.

Substituting (19) in the left-hand side of (3), we get

$$
\begin{aligned}
(\nabla_T^2+k^2)G=&\sum\sum\left[k^2-\frac{16\pi^2}{9a^2}(m^2+mn+n^2)\right]\\
&\cdot[A_{mn}T_1(x,y)+B_{mn}T_2(x,y)].
\end{aligned}
\tag{20}
$$

Since (17) and (20) are equal for all values of x and y we have by comparison

$$
A_{mn}=\frac{4j\omega\mu dT_1(x_0,y_0)}{16\sqrt{3}\,\pi^2(m^2+mn+n^2)-9\sqrt{3}\,a^2k^2} \tag{21}
$$

and

$$
B_{mn}=\frac{4j\omega\mu dT_2(x_0,y_0)}{16\sqrt{3}\,\pi^2(m^2+mn+n^2)-9\sqrt{3}\,a^2k^2}. \tag{22}
$$

Substituting (21) and (22) in (19), we have

$$
\begin{aligned}
G(x,y|x_0,y_0)=&4j\omega\mu d\\
&\cdot\sum_{-\infty}^{\infty}\sum_{-\infty}^{\infty}\frac{T_1(x_0,y_0)T_1(x,y)+T_2(x_0,y_0)T_2(x,y)}{16\sqrt{3}\,\pi^2(m^2+mn+n^2)-9\sqrt{3}\,a^2k^2}
\end{aligned}
\tag{23}
$$

which is the required Green's function for the equilateral triangle shown in Fig. 4(a).

A. Green's Functions for Even and Odd Modes

First term in the right-hand side of (23) corresponds to the Green's function for 30°–60° right-angled triangle given in (15).

The second term in (23) is the Green's function (divided by a factor of 2) for the odd mode of the equilateral triangle (i.e., a 30°–60° right-angled triangle shown in Fig. 3(a) with the side *OB* being an electric wall). This Green's function may be explicitly expressed as

$$G(x,y|x_0,y_0)=8j\omega\mu d \cdot \sum_{-\infty}^{\infty}\sum_{-\infty}^{\infty}\frac{T_2(x_0,y_0)T_2(x,y)}{16\sqrt{3}\,\pi^2(m^2+mn+n^2)-9\sqrt{3}\,a^2k^2}. \quad (24)$$

IV. Green's Functions for an Isosceles Right-Angled Triangle

As in earlier cases, additional line sources are placed outside the isosceles right-angled triangle shown in Fig. 5(a). The positions of the additional sources are shown in Fig. 5(b). In this case the right-hand side of (3), (after placing additional sources) reduces to

$$-\frac{j\omega\mu d}{2a^2}\sum_{-\infty}^{\infty}\sum_{-\infty}^{\infty}T(x_0,y_0)T(x,y) \quad (25)$$

where the potential function $T(x,y)$ is given by

$$T(x,y)=\cos\frac{m\pi x}{a}\cos\frac{n\pi y}{a}+(-1)^{m+n}\cos\frac{n\pi x}{a}\cos\frac{m\pi y}{a}. \quad (26)$$

The function $T(x,y)$ satisfies the boundary conditions (4) for this triangle of Fig. 5(a). As before, G can be expressed as

$$G=\sum_{-\infty}^{\infty}\sum_{-\infty}^{\infty}A_{mn}T(x,y). \quad (27)$$

The left-hand side of (3), then reduces to

$$\sum_{-\infty}^{\infty}\sum_{-\infty}^{\infty}A_{mn}\left[k^2-\left(\frac{m\pi}{a}\right)^2-\left(\frac{n\pi}{a}\right)^2\right]T(x,y). \quad (28)$$

The values of A_{mn} are obtained by equating (25) and (28). The Green's function is given by

$$G(x,y|x_0,y_0)=\sum_{-\infty}^{\infty}\sum_{-\infty}^{\infty}\frac{j\omega\mu dT(x_0,y_0)T(x,y)}{2\left[(m^2+n^2)\pi^2-a^2k^2\right]} \quad (29)$$

which is the required Green's function for an isosceles right-angle triangle shown in Fig. 5(a).

A. Green's Functions for Odd Mode

The odd-mode triangle for the present case has the same shape as shown in Fig. 5(a), with the side *OB* as an electric wall where (5) should be satisfied and the other sides are magnetic walls where (4) should be satisfied. Green's function for this case (dimensions and location unchanged as in Fig. 5(a)) is given by

$$G(x,y|x_0,y_0)=2j\omega\mu d\sum_{-\infty}^{\infty}\sum_{-\infty}^{\infty}\frac{U(x_0,y_0)U(x,y)}{\left[(m^2+n^2)\pi^2-4a^2k^2\right]} \quad (30)$$

where the summation is carried out only for odd values of m and n, and

$$U(x,y)=\cos\frac{m\pi x}{2a}\sin\frac{n\pi y}{2a}-(-1)^{(m+n)/2}\cos\frac{n\pi x}{2a}\sin\frac{m\pi y}{2a}. \quad (31)$$

Even mode of a right-angled isosceles triangle has the same shape as the original segment. Green's function given in (29) may be used for this case also.

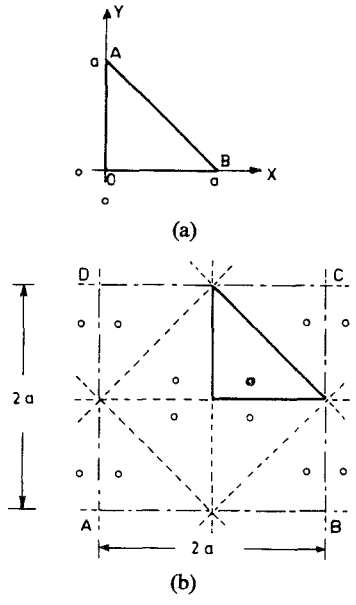

Fig. 5. (a) An isosceles right-angled triangular segment. (b) Location of image sources for an isosceles right-angled triangle.

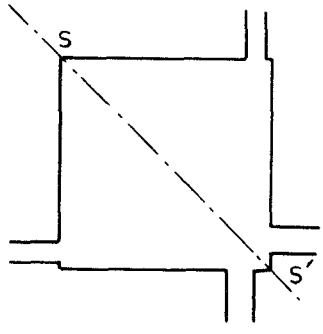

Fig. 6. A square planar segment with symmetry about the diagonal.

B. Green's Function when Hypotenuse is an Electric Wall

An isosceles right angled triangle, with the hypotenuse as an electric wall and the other two sides being magnetic walls, would need to be characterized for odd-mode analysis of a square having symmetry about one of its diagonals. For example, for the square planar segment shown in Fig. 6, the odd-mode triangle would be a right-angle isosceles shown in Fig. 5(a). For this case, the boundary condition (5) is valid on the hypotenuse *AB* and on the other two sides (4) is satisfied. In this case, the Green's function is found to be

$$G(x,y|x_0,y_0)=\sum_{m=-\infty}^{\infty}\sum_{n=-\infty}^{\infty}\frac{j\omega\mu dW(x_0,y_0)W(x,y)}{2\left[(m^2+n^2)\pi^2-a^2k^2\right]} \quad (32)$$

where

$$W(x,y)=\cos\frac{m\pi x}{a}\cos\frac{n\pi y}{a}-(-1)^{m+n}\cos\frac{n\pi x}{a}\cos\frac{m\pi y}{a}. \quad (33)$$

V. Concluding Remarks

The Green's functions reported in this paper may be used to analyze multiport circuits using triangular segments. Using segmentation method [3], other two dimensional shapes which can be divided into these three types of triangles (and rectangular and circular geometries) can also be analyzed.

The key step in the method used is the placement of additional image line sources and reduction of right-hand side of (3) to a periodic function. One of the factors in this representation, viz., $T_1(x, y)$ in (11), $T_2(x, y)$ in (17), $T(x, y)$ in (25), $U(x, y)$ in (30), and $W(x, y)$ in (32), is the potential function which satisfies the boundary conditions. Thus, this part of the procedure can be used in evaluation of potential functions in similar cases. This technique could also be used for finding Green's functions for triangular planar circuits with all short circuit boundaries [8]. A similar procedure can be used for finding Green's function for solution of Poisson's equation also.

References

[1] T. Okoshi and T. Miyoshi, "The planar circuit—An approach to microwave integrated circuitry," *IEEE Trans. Microwave Theory Tech.*, vol. MTT-20, pp. 245–252, Apr. 1972.

[2] P. Silvester, "Finite element analysis of planar microwave networks," *IEEE Trans. Microwave Theory Tech.*, vol. MTT-21, pp. 104–108, Feb. 1973.

[3] T. Okoshi, Y. Uehara, and T. Takeuchi, "The segmentation method—An approach to the analysis of microwave planar circuits," *IEEE Trans. Microwave Theory Tech.*, vol. MTT-24, pp. 662–668, Oct. 1976.

[4] J. Helszajn and D. S. James, "Planar triangular resonators with magnetic walls," *IEEE Trans. Microwave Theory Tech.*, vol. MTT-26, pp. 95–100, Feb. 1978.

[5] J. Helszajn, D. S. James, and W. T. Nisbet, "Circulators using planar triangular resonators," *IEEE Trans. Microwave Theory Tech.*, vol. MTT-27, pp. 188–193, Feb. 1979.

[6] P. M. Morse and H. Feshbach, *Methods of Theoretical Physics*. New York: McGraw-Hill, 1953, ch. 7, p. 812.

[7] Schelkunoff, *Electromagnetic Waves*. New York: Van Nostrand, 1943, p. 393.

[8] T. Okoshi and S. Kitazawa, "Computer analysis of short-boundary planar circuits," *IEEE Trans. Microwave Theory Tech.*, vol. MTT-23, pp. 299–306, Mar. 1975.

Letters

Addendum to "Closed-Form Expressions for the Current or Charge Distribution on Parallel Strips or Microstrip"

EDWARD F. KUESTER AND DAVID C. CHANG

It has been called to the authors' attention that (28) in the above paper[1] is too crudely approximated. The correct expression should read

$$C_m \cong \epsilon_r \frac{2l}{t} + \frac{2}{\pi}\left[\ln\left(\frac{2l}{t\sqrt{a_\epsilon}}\right) + 2(\epsilon_r + 1)\ln 2\right].$$

Manuscript received June 12, 1980; revised June 13, 1980.

The authors are with the Electromagnetics Laboratory, University of Colorado, Boulder, CO 80309.

[1] E. F. Kuester and D. C. Chang, *IEEE Trans. Microwave Theory Tech.*, vol. 28, pp. 254–259, March 1980.

Also, two further references on the subject have been discovered. Rochelle [1] gives an expression for C_p using only a constant trial function for $\rho(y)$. The error in the resulting formula can be as large as 5 percent, considerably larger than that obtainable from (14) of the subject paper. Shchapoval [2] has presented a variety of expressions valid for different ranges of l/t and ϵ_r for the capacitance as well as $\rho(y)$ of microstrip. In particular, he has obtained the limiting form of (20) of the paper in the case where $\epsilon_r \gg 1$.

References

[1] J. M. Rochelle, "Approximations for the symmetrical parallel-strip transmission line," *IEEE Trans. Microwave Theory Tech.*, vol. 23, pp. 712–714, 1975.

[2] E. A. Shchapoval, "Capacitance, inductance and effective relative permittivity of microstrip line," *Electron. Lett.*, vol. 11, pp. 225–226, 1975 (in Russian).

0018-9480/80/1000-1143$00.75 ©1980 IEEE